Simplified Numerical Tool for a Fast Strength Estimation of Squared Masonry Columns Reinforced with FRP Jackets

Luis C. M. da Silva[1(✉)], Ernesto Grande[2], and Gabriele Milani[1]

[1] Department A.B.C, Politecnico Di Milano, Piazza Leonardo da Vinci 32, 20133 Milan, Italy
{luiscarlos.martinsdasilva,gabriele.milani}@polimi.it
[2] University Guglielmo Marconi, Rome, Italy
e.grande@unimarconi.it

Abstract. The work addresses the retrofitting of masonry columns with fiber reinforced polymers (FRP) jackets. Experimentation is still at a higher level and the study tries to enrich the set of available numerical models to estimate the capacity of squared masonry columns with a periodic arrangement. The numerical procedure assumes a strain-based incremental formulation relying on equilibrium, compatibility, and kinematic equations and precluding strenuous integration of FEs. An elastic-perfectly plastic response with a Mohr-Coulomb failure criteria has been assumed for both brick units and mortar joints. Failure of the FRP is governed by limited tensile strength and tearing (in the corners of the columns). An associated plastic flow-rule is followed. The numerical strategy has been validated with data from several experimental campaigns, with existing literature approaches and code-based formulas. A good agreement has been found and the strategy demonstrated fast (1–2 s).

Keywords: Masonry columns · FRP jackets · Masonry compressive strength · Retrofit masonry columns

1 Introduction

Most existing masonry constructions have been built to withstand vertical loads. Unreinforced masonry tends to exhibit low tensile strength and quasi-brittle response, which somehow has determined its employment in structural elements whose stability is governed by compressive stresses [1–3]. From a logical extension, masonry compressive strength is then of utmost importance when designing and assessing the structural safety of such buildings. European normative EN 1052–1 [4] include principles for the experimental determination of masonry compressive strength (perpendicular to bed joints).

The construction and testing of stacked masonry prisms, or even larger setups, is yet found in the literature to estimate this property [5], as it allows a good correlation with results from code-based tests [5, 6]. To cope with the associated experimentation costs (and corresponding time), several alternatives have been presented in the literature

R. Capozucca et al. (Eds.): ICSCES 2022, LNCE 317, pp. 253–264, 2023.
https://doi.org/10.1007/978-3-031-24041-6_21

to assess the masonry compressive strength. These may be grouped in semi-empirical, analytical, or numerical approaches; however, these need to be validated by experimental data.

Semi-empirical laws, as the ones presented by Haseltine [7] and more recently by Sarhat and Sherwood [8] are used in masonry code provisions [9, 10]. Limited information is retrieved on the masonry response, but those allow giving a rational and conservative basis for design. On this regard, the pioneering work of Hilsdorf [11] led to important experimental contributions that nurtured the onset of novel formulations. Hilsdorf proposed that an applied uniaxial compression stress leads to a tri-axial stress state within the masonry; latter exploited by McNary and Abrams [7] who reported a comprehensive testing program for the tri-axial characterization of units and mortar. Analytical approaches that consider the effect of both masonry components have been then developed. A valuable research work has been presented by Drougkas et al. [12], in which a mechanistic-based micro-model was proposed. Results were compared with experimental data on compressed masonry elements and a promising accuracy was found. More sophisticated analysis, such as those retrieved from continuous Finite element (FE) method, have been also explored and with good results. For instance, the works from Brencich et al. [13], Shrive and Jessop [14] and Pina-Henriques and Lourenco [15].

Nowadays, it is generally consensual – with experimental evidence – that masonry compressive failure is governed by the interaction between units and mortar. Again, it bears stressing that this was especially due to Hilsdorf [11] disruptive idea, whose formulation has been later improved by Khoo and Hendry [16] to solve the limitation of assuming that units and mortar have a similar strain at failure. Perhaps due to the existing solid background on masonry compressive behavior, one can explain the unravel of new and exciting techniques being applied to this aim, as for instance machine learning-based methods [17]. Although the behavior of masonry under pure compression is well documented, the assessment of strengthened elements still deserves more insight. A typical retrofitting strategy is the use of composite materials such as FRP (Fiber-Reinforced Plastics). FRP material systems are composed of fibres within a polymeric matrix, being possible to mention, for instance, the use of reinforced polymers made from glass (GFRP), carbon (CFRP) and aramidic fibers (AFRP).

The present research focuses on the structural performance of masonry columns. Its behavior can be easily improved by adequate strengthening, such as the use of innovative materials as FRPs. Data retrieved from experimental works allow the development of analytical and numerical models to compute the confined strength. Although the confined compressive strength of masonry columns is typically obtained either via conservative empirical laws or experimental campaigns, numerical analysis can be also an alternative. Complex FE models may allow to reproduce compressive failure considering localization of deformation and damage propagation (with spitting and shear cracks). Nonetheless, the computational time required blurs its practicability, hence are seldom used in practice. In such a context, the present work intends to demonstrate a mechanistic-based approach that allows computing the confined compressive strength of masonry columns. The numerical model can reproduce the nonlinear behavior of masonry and the failure of

units, mortar, and composite wrap (with a polymeric base, such as FRP, GFRP, etc.). To circumvent the latter underlined concern, the strategy allows obtaining a solution in a pair of seconds and will be made available to extend its use to engineering design practice.

2 Simplified Numerical Model for Squared Masonry Columns

A numerical model to compute the compressive strength of squared masonry columns is proposed in this section. The main theoretical assumptions will be addressed, which include both the case of unreinforced and reinforced squared masonry columns and for the case of a periodic arrangement.

2.1 Unreinforced Squared Masonry Columns

A good basis of work is already present in the literature to characterize the compressive behaviour of unreinforced masonry [15]. From the pioneering work by Hilsdorf [11], it is well accepted today that masonry compressive failure is mainly governed by the interaction between units and mortar. In specific, it relies on the evidence that the compressive strength of brick units is higher than the one of mortar joints; and, in converse, that the lateral expansion given by the Poisson's ratio is higher for mortar joints in respect to brick units. In this regard, when a masonry column is subjected to a compressive load, the bed mortar joints tend to expand laterally. To fulfil the compatibility conditions, such deformation is restrained by units owing its lower deformability, thence leading to a pure tri-axial compression state in mortar joints and a compression-tension-tension state in brick units. Such behaviour is presented in Fig. 1.

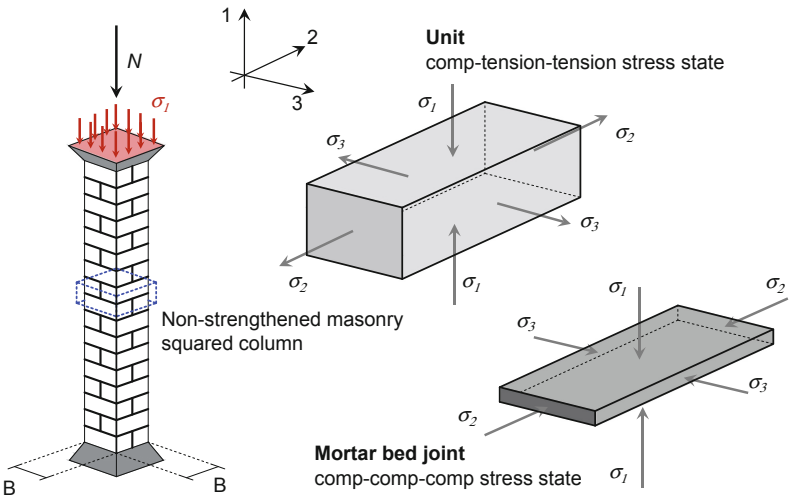

Fig. 1. Squared unreinforced masonry column and stress state in the masonry components.

2.2 FRP-Strengthened Squared Masonry Columns

Several experimental campaigns have been developed in literature in the use of modern and innovative interventions. In specific, the use of polymeric-based composites such as FRP (Fiber-Reinforced plastics) and GFRP (Glass-Fiber) are becoming a general solution. The adoption of such polymeric-based solutions allows increasing the ultimate capacity in terms of both strength and ultimate displacement.

Nonetheless, numerical works are still scarce and are typically based on complex micro-modelling approaches that have high cost in both modelling and processing stages [18]. Here, in order to decrease the required computational time costs, the numerical model is formulated accounting with the stress state addressed by Hilsdorf theory [11]. Regarding the latter, the model is enriched with kinematic compatibility conditions between masonry and the polymeric FRP wrap.

2.3 Constitutive Laws and Failure Criteria

A constitutive model based on an elastic-perfectly plastic assumption was considered for both masonry components. Failure of masonry components is governed by a Mohr-Coulomb behaviour. These assumptions are depicted in Fig. 2. In specific, the elastic limit for a given increment (i) is written such as:

$$f(\sigma_i) = \Delta\sigma_v^{(i)} - k = 0 \tag{1}$$

In which k defines the Mohr-Coulomb failure surface that, following the assumptions made, remains fixed in the stress space. For the polymeric-based and owing the high tensile strength and stiffness to weight ratio, an elastic behaviour with limited tensile strength was adopted:

$$\sigma_{FRP} = E\varepsilon_{FRP} \quad such\ that \quad \sigma_{FRP} \leq f_{t,FRP} \tag{2}$$

in which σ_{FRP}, ε_{FRP}, E_{FRP}, and $f_{t,FRP}$ are the tensile stress, tensile strain, Young's modulus, and tensile strength of the polymeric base, respectively (Fig. 2).

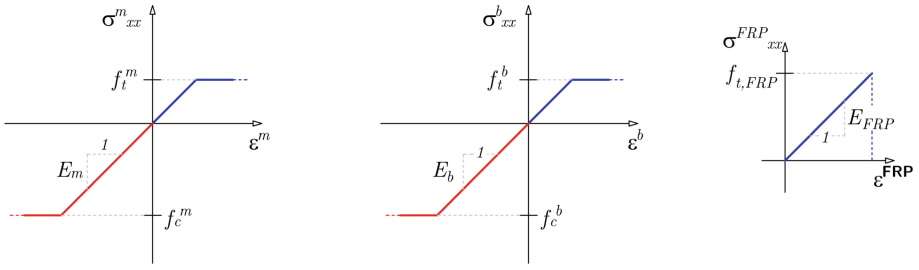

(a) mortar (b) brick (c) polymeric base (FRP)

Fig. 2. Constitutive models for materials.

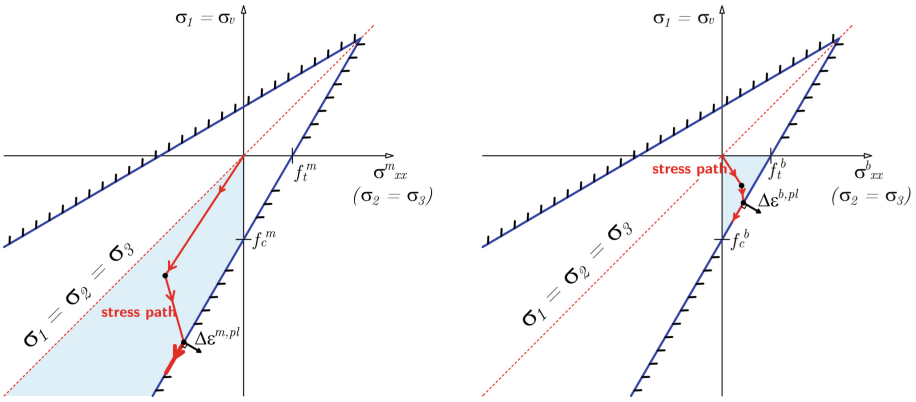

(a) mortar (b) brick

Fig. 3. Failure surface in the principal stress space (plane $\sigma_2 = \sigma_3$).

For both masonry components, an associated plastic flow rule has been assumed. In this regard, the plastic strain rate tensor for brick ($\Delta\varepsilon^{b,pl}$) and mortar ($\Delta\varepsilon^{m,pl}$) reads as:

$$\Delta\varepsilon^{(\cdot),pl} = \lambda_p^{(\cdot)} \frac{\partial f}{\partial \sigma_i} \quad i = 1, 2, 3 \; and \; (\cdot) = b, m \tag{3}$$

in which $(\Delta\varepsilon^{(\cdot)pl})^T = [\Delta\varepsilon_{xx}^{(\cdot)}, \Delta\varepsilon_v^{(\cdot)}]$. For the present numerical model, only one failure surface $f(\sigma_i)$ is active for each masonry component as depicted in Fig. 3.

2.4 (a) Computational Details

A brief presentation on the used compatibility, constitutive, and equilibrium equations are given herein. The formulation is written in a way that allows solving, through a vertical incremental strain approach, the solution to the unknown variables of the system. In specific, the system has a total of fifteen unknowns that are given next and depicted in Fig. 4.

$$\begin{cases} brick: \; \Delta\varepsilon_{xx}^{b}, \; \Delta\varepsilon_{v}^{b}, \; \Delta\sigma_{xx}^{b}, \; \Delta\lambda^{b}, \; \Delta\varepsilon_{xx}^{bpl}, \; \Delta\varepsilon_{v}^{bpl} \\ mortar: \; \Delta\varepsilon_{xx}^{m}, \; \Delta\varepsilon_{v}^{m}, \; \Delta\sigma_{xx}^{m}, \; \Delta\lambda^{m}, \; \Delta\varepsilon_{xx}^{mpl}, \; \Delta\varepsilon_{v}^{mpl} \\ FRP: \; \Delta\sigma_{FRP}, \; \Delta\varepsilon_{FRP} \\ load: \; \Delta\sigma_{v} \end{cases} \tag{4}$$

In which $\Delta\varepsilon_{xx}^{b}$ and $\Delta\varepsilon_{xx}^{m}$ are the horizontal elastic strain increments for brick and mortar; $\Delta\varepsilon_{v}^{b}$ and $\Delta\varepsilon_{v}^{m}$ are the vertical elastic strain increments for brick and mortar, respectively. Following an additive decomposition for strain terms, thence $\Delta\varepsilon_{xx}^{bpl}$, $\Delta\varepsilon_{v}^{bpl}$ are the corresponding plastic strain increments for brick; and $\Delta\varepsilon_{xx}^{mpl}$, $\Delta\varepsilon_{v}^{mpl}$ the corresponding plastic strain increments for mortar joints. The stress quantities are expressed using a similar notation, such that $\Delta\sigma_{xx}^{b}$ and $\Delta\sigma_{xx}^{m}$ are the horizontal stress in brick and

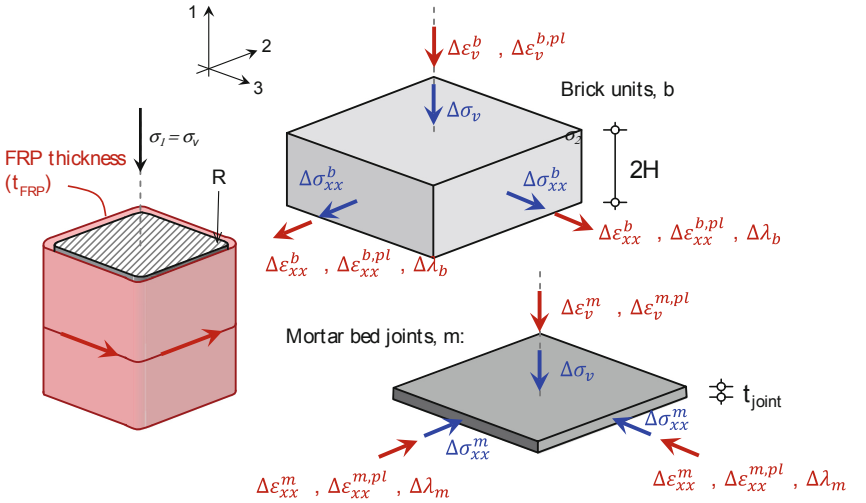

Fig. 4. Description of the geometric parameters and the stress-state components for the FRP-strengthened masonry column.

mortar bed joint, being $\Delta\lambda^b$ and $\Delta\lambda^m$ the corresponding plastic multipliers. The elastic strain and stress values in the FRP wrap are defined by $\Delta\sigma_{FRP}$ and $\Delta\varepsilon_{FRP}$, respectively.

Constitutive relations are defined for both brick and mortar according to:

$$[\Delta\varepsilon_{xx}^{(\cdot)},\ \Delta\varepsilon_v^{(\cdot)}]^T = \frac{1}{E_{(\cdot)}}\begin{bmatrix} 1 - v_{(\cdot)} & -v_{(\cdot)} \\ -2v_{(\cdot)} & 1 \end{bmatrix}\begin{bmatrix} \Delta\sigma_{xx}^{(\cdot)} \\ \Delta\sigma_v^{(\cdot)} \end{bmatrix} \quad (\cdot) = b, m \tag{5}$$

In which the plastic relations for the masonry components are described through an associated plastic flow rule such that, following the assumptions ascribed in Sect. 2.3, one finds:

$$\begin{cases} \Delta\varepsilon_{xx}^{(\cdot),pl} = \Delta\lambda_{(\cdot)}\frac{f_{c(\cdot)}}{f_{t(\cdot)}} \\ \Delta\varepsilon_v^{(\cdot),pl} = -\Delta\lambda_{(\cdot)} \end{cases} \tag{6}$$

Compatibility relations between the bed joint and brick interface in the horizontal and vertical directions are, respectively, given as:

$$\Delta\varepsilon_{xx}^b + \Delta\varepsilon_{xx}^{b,pl} = \Delta\varepsilon_{xx}^m + \Delta\varepsilon_{xx}^{m,pl} \tag{7}$$

$$\Delta\varepsilon_v(2H + t) = 2H(\Delta\varepsilon_v^b + \Delta\varepsilon_v^{b,pl}) + t(\Delta\varepsilon_v^m + \Delta\varepsilon_v^{m,pl}) \tag{8}$$

and between the polymer wrap with the brick surface as:

$$\Delta\varepsilon_{xx}^b + \Delta\varepsilon_{xx}^{b,pl} = \Delta\varepsilon_{FRP} \tag{9}$$

The increment of stress in the masonry components is, for the current iteration i, given as:

$$\Delta\sigma_v^{(i)} = \frac{f_{c(\cdot)}}{f_{t(\cdot)}}\Delta\sigma_{xx}^{(\cdot)\,(i)} - f_{c(\cdot)} - \sigma_v^{i-1} + \frac{f_{c(\cdot)}}{f_{t(\cdot)}}\sigma_{xx}^{(\cdot)\,(i-1)} \tag{10}$$

and for the polymeric wrap:

$$\Delta\sigma_{FRP} = E_{FRP}\Delta\varepsilon_{FRP} \tag{11}$$

Being the global equilibrium in the horizontal direction guaranteed if:

$$2HB\Delta\sigma_{xx}^{b} + tB\Delta\sigma_{xx}^{m} + t_{FRP}(2H + t)\sigma_{FRP} = 0 \tag{12}$$

The uncertainty of the mechanical properties of masonry components is generally significant. This is well document in experimental campaigns and, therefore, uncertainty is also modelled through a forward propagation approach. Coefficient of variation (Cov) values are eligible to be assigned to each mechanical parameter, for which the numerical model may provide results of a lower bound, a mean value, and an upper bound.

3 Experimental Data for Validation

The accuracy of the proposed numerical model is evaluated based on two experimental campaigns. In particular, the works from Faella et al. [19] and Krevaikas et al. [20] on the strengthening of squared masonry columns were selected. The results are provided in terms of ultimate capacity for both non-strengthened and strengthened cases, and values retrieved from the expressions of Eurocode 6 [10], ACI [9] and Italian code [21] are also presented.

The works selected from Faella et al. [19] gather tests on 28 clay-brick masonry squared columns confined by 1 or 2 layers of GFRP. The test series is indicated with the letter 'B' and are made with two different cross-sections equal to 380x380 mm^2 and to 250x250 mm^2, as indicated in Table 1. The masonry prisms were casted with weak mortar, composed by pozzolan, with low compression strength and that tries to reproduce a mortar type used in historical buildings in the Mediterranean area.

Table 1. Experimental tests from Faella et al. [19].

Test code	B (mm)	R (mm)	t_{mortar} (mm)	tlayer,wrap (mm)	$n_{layers,wrap}$	EFRP (MPa)	ft,FRP (MPa)
B#01UR	371.5	25	10	–	–	–	–
B#02UR	377.5	25	10	–	–	–	–
B#03UR	371	25	10	–	–	–	–
B#04G1	381.5	25	10	0.23	1	65000	1600
B#05G1	381	25	10	0.23	1	65000	1600
B#06G1	378.5	25	10	0.23	1	65000	1600
B#07G2	380.5	25	10	0.23	2	65000	1600
B#08G2	377.5	25	10	0.23	2	65000	1600

(*continued*)

Table 1. (*continued*)

Test code	B (mm)	R (mm)	t_{mortar} (mm)	tlayer,wrap (mm)	$n_{layers,wrap}$	EFRP (MPa)	ft,FRP (MPa)
B#09G2	378.5	25	10	0.23	2	65000	1600
B#10UR	244	25	10	–	–	–	–
B#11UR	243.5	25	10	–	–	–	–
B#12UR	244	25	10	–	–	–	–
B#13G1	249	25	10	0.23	1	65000	1600
B#14G1	249.5	25	10	0.23	1	65000	1600
B#15G1	248.5	25	10	0.23	1	65000	1600
B#16G2	247.5	25	10	0.23	2	65000	1600
B#17G2	246.5	25	10	0.23	2	65000	1600
B#18G2	248.5	25	10	0.23	2	65000	1600
B#19UR	250	10	10	–	–	–	–
B#20UR	250	10	10	–	–	–	–
B#21G1	250	10	10	0.48	1	80700	2560
B#22UR	250	10	10	–	–	–	–
B#23UR	250	10	10	–	–	–	–
B#24UR	250	10	10	–	–	–	–
B#25G1	250	10	10	0.48	1	80700	2560
B#26G1	250	10	10	0.48	1	80700	2560
B#27G2	250	10	10	0.48	2	80700	2560
B#28G2	250	10	10	0.48	2	80700	2560

For brick units, and considering the experimental information available, an E_b = 15000 MPa, v_b = 0.15, f_{cb} = 17.5 MPa (CoV = 15%) and f_{tb} = 1.75 MPa (CoV = 15%) were assumed.

Similarly, for mortar it was considered E_m = 1000 MPa, v_m = 0.3, f_{cm} = 1.027 MPa (CoV = 15%), f_{tm} = 0.1027 MPa (CoV = 15%).

The works selected from Krevaikas et al. [20] gather tests on 8 clay-brick masonry squared columns confined by 1,2,3 or 5 layers of polymeric-wrap. In specific, the clay brick masonry was strengthened with a carbon and glass-based fiber polymer. The tests series are indicated with the letter 'C' and are made with a cross-section of 115x115 mm^2, as indicated in Table 2. For brick units, and considering the experimental information available, a E_b = 15000 MPa, v_b = 0.15, f_{cb} = 23.5 MPa (CoV = 15%) and f_{tb} = 2.35 MPa (CoV = 15%) were assumed. Similarly, for mortar it was considered E_m = 300 MPa, v_m = 0.3, f_{cm} = 2.85 MPa (CoV = 15%), f_{tm} = 0.285 MPa (CoV = 15%). The CoV values are assumed in this study.

Table 2. Experimental tests from Krevaikas et al. [20].

Test code	B (mm)	R (mm)	t_{mortar} (mm)	tlayer,wrap (mm)	$n_{layers,wrap}$	EFRP (MPa)	ft,FRP (MPa)
C1_1_R10	115	10	10	0.118	1	23000	3500
C1_1_R20	115	20	10	0.118	1	23000	3500
C2_1_R10	115	10	10	0.118	2	23000	3500
C2_1_R20	115	20	10	0.118	2	23000	3500
C3_1_R20	115	10	10	0.118	3	23000	3500
C3_1_R20	115	20	10	0.118	3	23000	3500
G5_1_R10	115	10	10	0.183	5	70000	2000
G5_1_R20	115	20	10	0.183	5	70000	2000

The results for the Faella et al. [19] and Krevaikas et al. [20] tests are provided in Fig. 5. Regarding the former, the experimental data fits well with the envelope of the proposed numerical model. Larger differences are yet found for the last four batches, i.e. for the squared column strengthened with Glass-fiber polymer. Nonetheless, the proposed model offers a conservative margin. Results from the Eurocode 6 [10] and ACI formulas [9] are too conservative for all the un-strengthened cases. On the other hand, the IT CNR DR 200 (2004) [21] leads to good estimations for the strengthened batches (when assuming the following parameters $\alpha_1 = 0.5$, $\alpha_2 = 1.0$ and $\alpha_3 = 1.0$).

Concerning the latter, the numerical results lead to good estimations with the data from Krevaikas et al. [20]. The larger discrepancy is related with the C21R10 batch (~26%).

In general, the model fits well, even in the absence of adequate measures for the COV values. In this case, the IT CNR DR 200 (2004) normative is too conservative (when assuming the following parameters $\alpha_1 = 0.5$, $\alpha_2 = 1.0$ and $\alpha_3 = 1.0$).

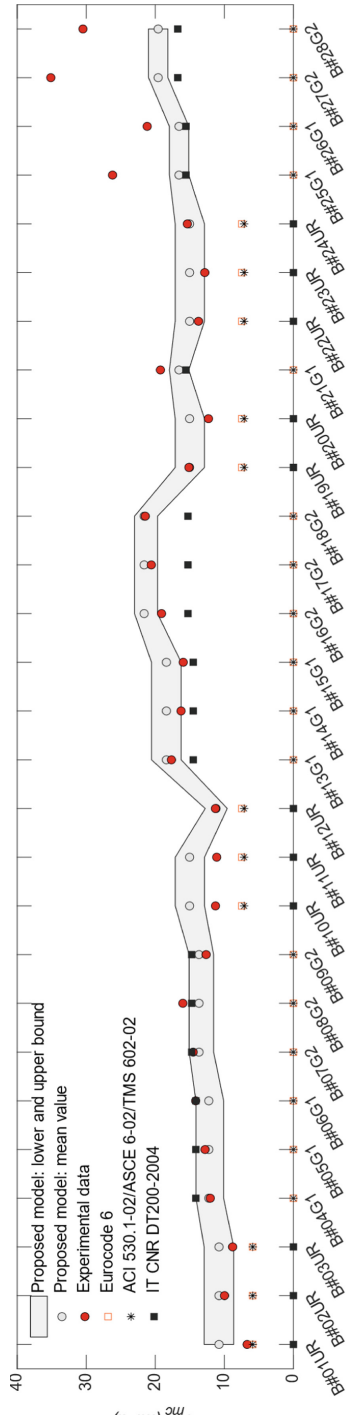

(a) *Faella et al. (2011)*

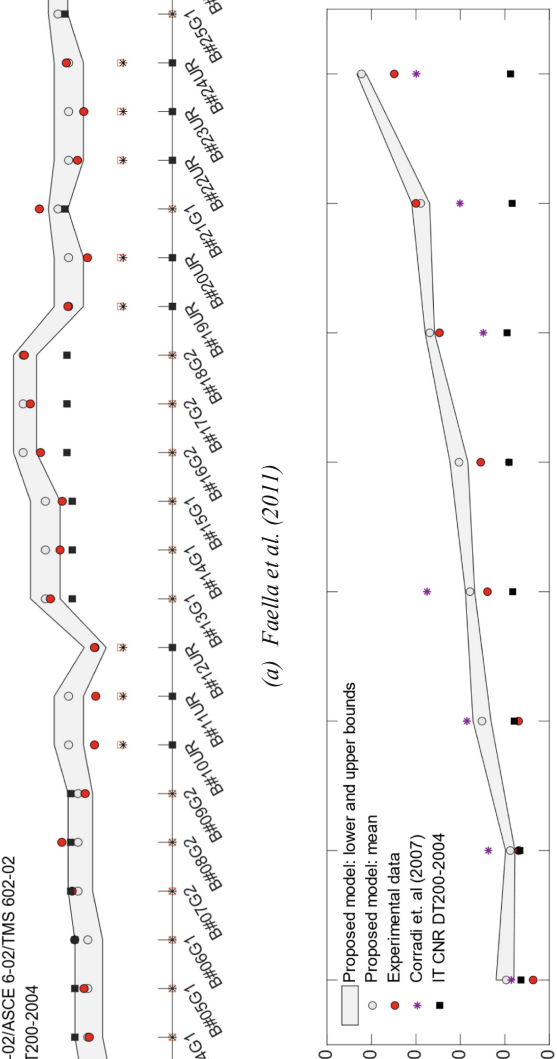

(b) *Krevaikas et al. (2005)*

Fig. 5. Comparison between the numerical results against with experimental data.

4 Conclusions

The tensile low strength and quasi-brittle response characterizes the typical behavior of unreinforced masonries. These features somehow determined the employment of masonry in structural elements whose stability is governed by compressive stresses. Although the behavior of masonry under pure compression is well documented, the assessment of strengthened elements still deserves better comprehension. This need led to the development of a simple numerical model, based on the Hilsdorf's assumptions, which allows giving estimations on the capacity of squared masonry columns. Both unstrengthened and strengthened columns, i.e. with polymeric-based composites such as FRP (Fiber-Reinforced plastics) and GFRP (Glass-Fiber), are considered. The numerical model provides solutions within two seconds, and the results fit well with experimental data collected from clay-brick masonries. The importance of propagating uncertainty has been also demonstrated, especially since the compressive strength of brick units has generally a high CoV value. The numerical tool can be put at disposal to the community especially for retrofitting studies. Several improvements to the model can be also addressed, such as the adding of a cap in compression within the failure criteria for mortar joints, and the modification of the failure criteria for bricks, i.e. to a so-called Modified Mohr-Coulomb criteria.

References

1. Lourenço, P.B., Silva, L.C.: Computational applications in masonry structures: from the meso-scale to the super-large/super-complex. Int. J. Multiscale Comput. Eng. **18**(1), 1–30 (2020). https://doi.org/10.1615/IntJMultCompEng.2020030889
2. Funari, M.F., Silva, L.C., Mousavian, E., Lourenço, P.B.: Real-time structural stability of domes through limit analysis: application to St. Peter's Dome. Int. J. Archit. Herit., 1–23 (2021). https://doi.org/10.1080/15583058.2021.1992539
3. Funari, M.F., Silva, L.C., Savalle, N., Lourenço, P.B.: A concurrent micro/macro FE-model optimized with a limit analysis tool for the assessment of dry-joint masonry structures. Int. J. Multiscale Comput. Eng. **20**(5), 65–85 (2022). https://doi.org/10.1615/IntJMultCompEng.2021040212
4. CEN. EN 1052–1. Methods of test for masonry – Part 1: Determination of compressive strength. Brussels, Belgium (1999)
5. Mojsilović, N.: Strength of masonry subjected to in-plane loading: a contribution. Int. J. Solids Struct. **48**(6), 865–873 (2011). https://doi.org/10.1016/j.ijsolstr.2010.11.019
6. Fortes, E.S., Parsekian, G.A., Fonseca, F.S.: Relationship between the compressive strength of concrete masonry and the compressive strength of concrete masonry units. J. Mater. Civ. Eng. **27**(9), 4014238 (2015). https://doi.org/10.1061/(ASCE)MT.1943-5533.0001204
7. Haseltine, B.: International rules for masonry and their effect on the UK. Mason. Int. **1**(2), 41–43 (1987)
8. Sarhat, S.R., Sherwood, E.G.: The prediction of compressive strength of ungrouted hollow concrete block masonry. Constr. Build. Mater. **58**, 111–121 (2014). https://doi.org/10.1016/j.conbuildmat.2014.01.025
9. ACI, ACI 530.1–02. Commentary on specification for masonry structures. Manual of concrete practice. Detroit, USA (2004)
10. EN 1996–1–1, Eurocode 6: design of masonry structures. Part 1–1: general rules for reinforced and unreinforced masonry structures (2005)

11. Hilsdorf, H.K.: Investigation into the failure mechanism of brick masonry loaded in axial compression. Designing, engineering and constructing with masonry products. Gulf Publ. Co., pp. 34–41 (1969)
12. Drougkas, A., Roca, P., Molins, C.: Nonlinear micro-mechanical analysis of masonry periodic unit cells. Int. J. Solids Struct. **80**, 193–211 (2016). https://doi.org/10.1016/j.ijsolstr.2015.11.004
13. Brencich, A., Corradi, C., Gambarotta, L., Mantegazza, G., Sterpi, E.: Compressive strength of solid clay brick masonry under eccentric loading. In: Proceeding of British Masonry Society, pp. 37–46 (2002)
14. Shrive, N.G., Jessop, E.L.: An examination of the failure mechanism of masonry piers, prisms and walls subjected to compression. In: Proceeding of British Ceramic Society, pp. 30–110–7 (1982)
15. Lourenço, P.B., Pina-Henriques, J.: Validation of analytical and continuum numerical methods for estimating the compressive strength of masonry. Comput. Struct. **84**(29), 1977–1989 (2006). https://doi.org/10.1016/j.compstruc.2006.08.009
16. Khoo, C., HEndry, A.: A failure criterion for brickwork in axial compression. In: Proceeding of the 3rd International Brick/Block Masonry Conference, pp. 139–145 (1973)
17. Asteris, P.G., et al.: Masonry compressive strength prediction using artificial neural networks, pp. 200–224 (2019)
18. Scacco, J., Ghiassi, B., Milani, G., Lourenço, P.B.: A fast modeling approach for numerical analysis of unreinforced and FRCM reinforced masonry walls under out-of-plane loading. Compos. Part B Eng. **180**(107553) (2020). https://doi.org/10.1016/j.compositesb.2019.107553
19. Faella, C., et al.: Masonry columns confined by composite materials: experimental investigation. Compos. Part B Eng. **42**(4), 692–704 (2011). https://doi.org/10.1016/j.compositesb.2011.02.001
20. Krevaikas, T.D., Triantafillou, T.C.: Masonry confinement with fiber-reinforced polymers. J. Compos. Constr. **9**(2), 128–135 (2005). https://doi.org/10.1061/(ASCE)1090-0268(2005)9:2(128)
21. CNR-DT200 R1/2012. Guide for design and construction of externally bonded FRP systems for strengthening existing structures : materials, RC and PC structures, masonry structures (2006)